MM Science Journal | www.mmscience.eu
ISSN 1803-1269 (Print) | ISSN 1805-0476 (On-line)
Special Issue | CUTTING TOOLS 2024
1st International Conference on Cutting Tools
November 20-22, 2024, Trnava, Slovakia
DOI: 10.17973/MMSJ.2025_03_2025012

CUTTINGTOOLS2024-00002

OPTIMIZATION OF PARAMETERS IN ROBOTIC ADDITIVE MANUFACTURING OF THIN-WALLED TUBES: EXPERIMENTAL ANALYSIS AND PATH PLANNING

M. Csekei[1]*, J. Sido[1], P. Niznan[1], R. Ruzarovsky[1], R. Zelnik[1], D. Michal[1]
[1]Slovak University of Technology in Bratislava, Faculty of Materials Science and Technology in Trnava, Institute of Production Technologies, Trnava, Slovakia
*martin.csekei@stuba.sk

Abstract
Robotic Additive Manufacturing (RAM) represents an innovative approach to 3D printing, utilizing multi-axis industrial robots to execute complex printing tasks. This study focuses on path planning and the investigation of key parameters affecting the print quality of thin-walled tubes printed using a planar method. The experiments analyzed the effects of cooling, robot movement speed, material feed rate, and the number of perimeter layers on print quality. The results indicate that the combination of these parameters influences the quality and overall success of the printing process. Path generation was based on G-code created in open-source slicers, which was adapted for the ABB IRB 120 industrial robot. Future research will focus on expanding the study to the printing of non-planar curved tubes.

Keywords:
Robotic Additive Manufacturing, Industrial Robot, 3D Printing, Path Planning, Thin-Walled Tubes

1 INTRODUCTION

Additive Manufacturing (AM) is a modern manufacturing process that enables the creation of objects through the layer-by-layer deposition of material, with each layer generated based on a digital model [Rasiya 2020]. Ongoing research in the field of additive manufacturing has led to the development of new technologies and applications, significantly expanding its use across various industrial sectors [Abdulhameed 2019]. One of these innovative technologies is Robotic Additive Manufacturing (RAM) [Shah 2022].

Robotic Additive Manufacturing (RAM) combines the capabilities of multi-axis industrial robots with additive manufacturing technologies, particularly their extrusion systems (printing heads) [Kubalak 2016]. Industrial robots are characterized by high speed, precision, payload capacity, repeatability, and, most importantly, greater motion flexibility compared to conventional additive manufacturing equipment [Singh 2022]. The integration of these robotic arm characteristics with the advantages of traditional additive manufacturing opens new possibilities for producing geometries and shapes that were previously unattainable using conventional subtractive methods or standard 3D printing [Fry 2020].

In the case of traditional 3D printers, the process of motion generation and process parameter settings is typically executed using commercial software solutions [Bryła 2021]. These systems commonly utilize G-code, which is generated based on a digital 3D-CAD model sliced into 2D layers within so-called "slicer" software [Sljivic 2019]. However, robotic additive manufacturing enables more flexible path planning, which depends on the specific printing method used [Geuy 2023]. The standard approaches include:

- Generation of 2D planar (flat) layers.
- Generation of 3D non-planar (curved) layers.

The generation of 2D planar layers, which are positioned within a single X-Y plane, has been extensively studied by researchers in the context of traditional 3D printers. This approach is well-suited for Cartesian 3D printers; however, when applied to industrial robots, it often fails to leverage the full potential of this technology [Hajare 2022].

On the other hand, 3D non-planar layers generated across multiple planes are particularly well-suited for 6-axis industrial robots. This approach frequently involves adaptive adjustments to the orientation of the print head during the printing process, enabling the execution of advanced additive manufacturing tasks such as printing on curved surfaces [Li 2024], smoothing staircase effects with conformal layers [Safeea 2022], printing thin-walled curved tubes [Bhatt 2020] and fabricating lattice structures [Huang 2019].

Before implementing advanced printing tasks, it is essential to thoroughly configure and optimize all printing process parameters, with initial testing recommended on planar printing tasks. This study utilizes an ABB industrial robot as an experimental platform to validate the proposed methods and strategies [Miri 2022].

2 METHODOLOGY

This paper focuses on robotic additive manufacturing of thin-walled tubes formed by planar layers and the investigation of key parameters affecting the successful execution of the printing task. The system architecture and fundamental methodology are illustrated in Figure 1.

2.1 Path planning – G-code generation

In this study, path planning was conducted through G-code generation. The process began with a 3D-CAD model, which was sliced using open-source slicer software. It was essential to configure all relevant parameters, such as nozzle diameter, layer height, infill pattern and density, as well as the number of bottom, top, and perimeter layers.

In conventional 3D printing, parts are typically printed with infill and a defined number of top and bottom layers. However, for thin-walled structures, an alternative strategy can be applied, where the entire 3D-CAD model is used, but the infill is set to 0%, and both top and bottom layers are disabled. By setting the infill to 0% when using a solid 3D CAD model, only the perimeter paths are planned and subsequently printed (Fig. 3 a, c). The number of perimeter layers can be set to one or more, depending on the desired wall thickness and the number of contour lines.

In this study, the parameters were tested by printing a cylindrical sample with a diameter of Ø30 mm and a height of 40 mm. The configured slicer parameters are summarized in Table 1.

2.2 Creation of the Digital Model of the Station

Digital model of the experimental station was developed using RobotStudio software to configure motion parameters, generate robotic movements and simulate the entire printing process. The digital model was equipped with the same industrial robot (ABB IRB 120), a printing head and other essential components required for the execution of the printing process, mirroring the real experimental setup. A critical aspect of the digital model creation was the precise definition of the WorkObject, which represents the printing position with accurately determined coordinates. This ensured that the robot could follow the planned printing paths with high precision while avoiding potential collisions during the process.

2.3 Motion generation

The G-code, which is traditionally used for standard 3-axis 3D printers, had to be adapted for implementation with an industrial robot. By utilizing the 3D Printing PowerPac add-in, it was possible to integrate the G-code into the virtual station. If necessary, the number of print points could be reduced to optimize the process. Beyond integrating the G-code, it was essential to define all additional motion parameters for the industrial robot. These parameters included the robot's movement speed, zone settings, tool head orientation, and other factors necessary for ensuring the proper execution of the printing process. Through this approach, robot movements were generated with precisely defined motion parameters, ensuring the accurate execution of the additive manufacturing process.

2.4 Real Experimental Station

The ABB IRB 120 industrial robot was used for the implementation of the robotic additive manufacturing. This robot was equipped with a modified FDM (Fused Deposition Modeling) print head for processing thermoplastic material in the form of filament. The experimental workstation included an integrated print bed, serving as a build platform for depositing individual layers of the final 3D-printed product.

Using the FlexPendant controller of the industrial robot, the precise printing position (WorkObject) and the tool center point (TCP) of the real print head were accurately defined. These configurations enabled precise motion control of the robot, ensuring seamless synchronization between the robot's movements and the printing process.

2.5 Extruder control

The print head was controlled by a custom-developed control system, enabling precise regulation of its process parameters. A Bigtreetech BTT SKR V1.4 motherboard, originally designed for conventional 3D printers, was utilized and connected to a Raspberry Pi 4 Model B as the control computer.

To enhance monitoring and control capabilities, a customized web-based interface was developed, allowing real-time supervision and adjustment of key functions of the print head. The main control processes included heating the print head to the desired temperature, fan control and extrusion control.

2.6 Integration of complete print path

Once the complete printing path was generated, it was transferred to the control unit of the industrial robot. To facilitate this process, the 3D Printing PowerPac add-in was installed in the robot's control unit, enabling the processing and interpretation of the G-code generated for printing. The communication between the industrial robot and the computer was established via an Ethernet connection.

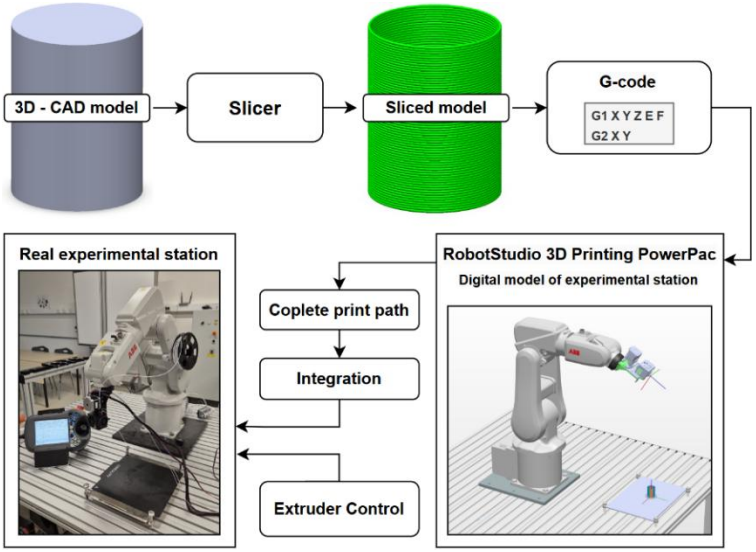

Fig. 1: System architecture and fundamental methodology of Robotic Additive Manufacturing

3 RESULTS AND DISCUSSION

For the series of experiments focused on the printing of thin-walled tubes, the experimental station described in Chapter 2 was utilized. Throughout all experiments, the same hardware configuration was maintained to ensure consistent test conditions. The hardware specifications and components are detailed in Table 1.

Tab. 1: Experimental hardware and software

Item	Description
Robot	ABB IRB120
Extruder	Modified Extruder for Creality Ender 3
Nozzle	1mm
Material extrusion	Constant, continuous
Fans	2
Print bed	Magnetic, non-heated
Slicer (E2)	UltiMaker CURA, Prusa Slicer

The constant and variable parameters used for print path configuration in individual printing experiments are summarized in Table 2. These parameters facilitated a detailed analysis of how specific settings influence the quality and efficiency of the additive manufacturing process. Constant parameters ensured stability and repeatability across all experiments, allowing for reliable comparisons. Variable parameters enabled the investigation of their direct impact on the final printed product, providing insights into optimal process settings.

Tab. 2: constant and variable parameters of experiments

Parameter	Con/Var	Setup
Material	Constant	PLA
Material diameter	Constant	1,75 mm
Extrusion temp.	Constant	210 °C
Nozzle size	Constant	1mm
Nozzle type	Constant	Extended
Layer height	Constant	0,5 mm
Infill	Constant	No
Fan – heatbreak	Constant	Off
Fan – nozzle (E1)	Variable	Off, 20%, 50%, 100%
Motion speed (E3)	Variable	v10, v20, v30, v0
Perimeter (E4)	Variable	1, 2, 4 perimeters

The modified parameters used in individual experiments, along with their results, are shown in the following sections. This section provides a comprehensive overview of how various process settings influenced print quality and the performance of the robotic additive manufacturing process. Additionally, photographs of the printed experimental samples are included to visually demonstrate the effects of different parameter configurations on the final printed structures.

3.1 Experiment 1 – Fan

FDM/FFF print heads are typically equipped with cooling systems utilizing fans. The print head used in our experimental setup is equipped with two fans. The first fan is responsible for cooling the cold end and the heatbreak, which is a part of the extruder that prevents heat transfer from the hot end to the upper sections of the extruder and helps regulate material flow. The second fan cools the extruded material exiting the nozzle and controls its solidification. The operation of the fans, including turning them on and off or adjusting their speed in percentage (%), was managed through the print head control software.

For printing tasks involving internal infill, cooling is often set to lower values or, in some cases, completely turned off. In this experiment, the cooling of the heat break was entirely deactivated. The cooling of the nozzle and the extruded material was tested in four modes: 1. completely off (0%), 2. set to 20%, 3. set to 50%, and 4. set to 100%. Testing was conducted at a constant robot movement speed of V30 (30 mm/s).

The results of the experiment, including print quality and the impact of different fan settings on material solidification, are shown in Figure 2. These results provide insight into the effect of cooling on robotic additive manufacturing of thin-walled tubes and help optimize parameters for achieving the best possible print quality.

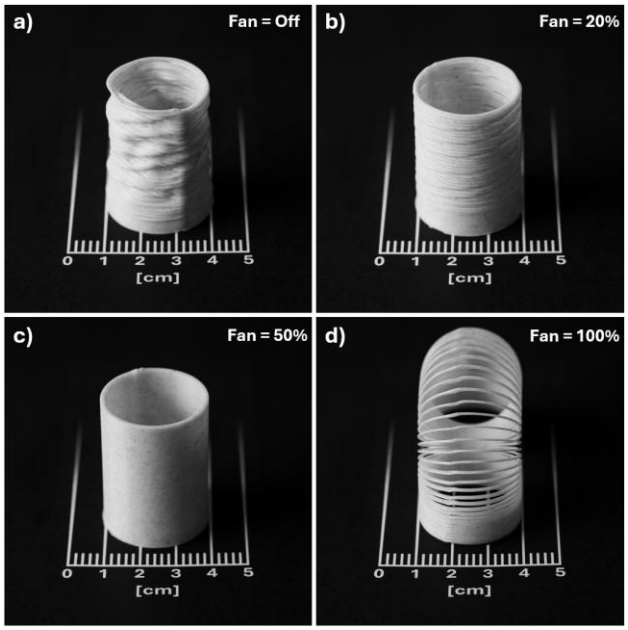

Fig. 2: Experiment 1 – FAN results
a) FAN = off, b) Fan = 20%, c) Fan = 50%, d) Fan = 100%

When printing thin-walled components, cooling of the extruded material is typically essential to ensure sufficient solidification. At completely disabled or low 20% cooling, the lower layers sagged, and the subsequent layers exhibited waviness. This resulted in significant inaccuracies in the deposited layers (Fig. 2 a, b). This phenomenon is particularly pronounced in smaller components, where individual layers do not have enough time to solidify properly. A high level of cooling caused excessively rapid solidification of the extruded material, leading to complete delamination of the individual layers (Fig. 2 d). The best surface quality of the printed sample was achieved at a fan power setting of 50%, where no delamination occurred, even under applied force. The applied force was manually exerted by hand to assess the layer adhesion, without any precise quantification or experimental measurement.

3.2 Experiment 2 – Seam

For path planning in robotic additive manufacturing, where movements are generated from G-code, various open-source slicers can be used for G-code generation. These slicers offer different settings for the so-called "seam" – the transition between layers during printing.

Seam paths are typically travel moves during which extrusion is either turned off or retraction is enabled. The seam can also be generated along sharp edges of the printed object, ensuring minimal visibility on the part's surface. When using a print head with continuous material

feeding, without the ability to disable extrusion during the print job, and when printing rotational parts without side edges, careful adjustment of the seam position and travel paths was necessary.

With the UltiMaker CURA slicer, the seam was automatically generated for a solid cylinder (Fig. 3 a)), and its position could be adjusted. However, despite testing various settings, it was not possible to achieve a completely consistent X and Y position of the seam (Fig. 3 c)). Additionally, the travel moves of the seam were directed inward (Fig. 3 e)), causing unwanted effects on the print quality (Fig. 4 a)).

This issue was addressed by modifying the CAD model to include only the outer shell of the cylinder – a hollow cylinder (Fig. 3 b)). This modification eliminated internal travel moves (Fig. 3 f)), however, even with this configuration, achieving a fully consistent X and Y seam position was not possible (Fig. 3 d)). Another issue with this configuration was the slicer's behaviour, where some paths were generated in a clockwise direction and others in a counterclockwise direction. This phenomenon can significantly affect the mechanical properties in the seam area, which is critical for the quality and strength of the printed object.

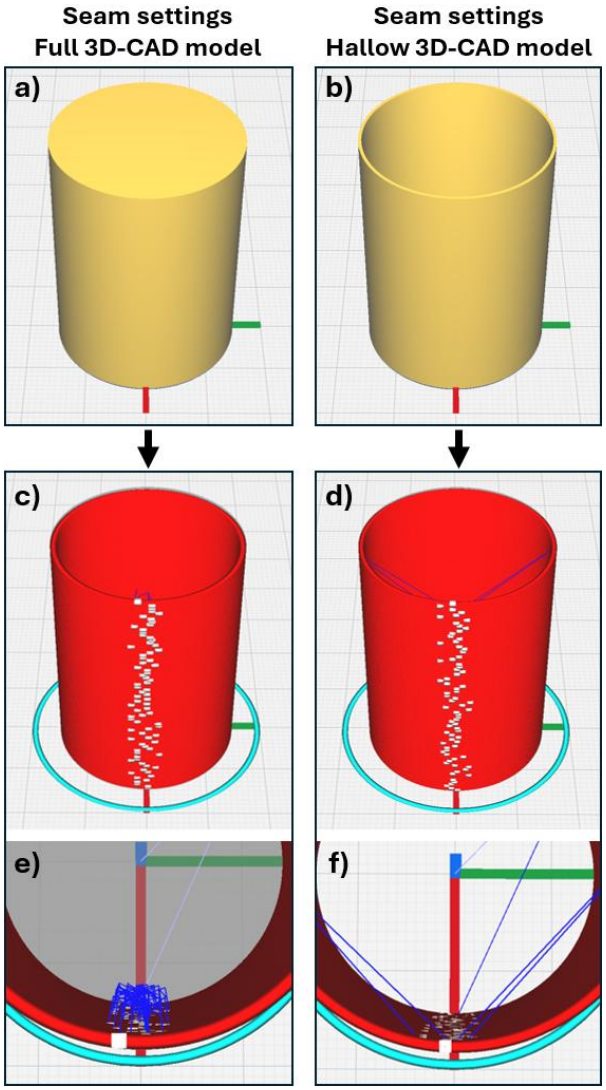

Fig. 3: Seam settings in UltiMakerCura Slicer
a) Full 3D – CAD model, b) Hallow 3D – CAD model
c), d) X and Y seam position, c), f) robot travel motions

Prusa Slicer proved to be an exceptionally suitable tool for seam configuration in the printing of thin-walled tubes. This slicer allows simple and precise seam positioning for each layer, ensuring that it is located at a 100% identical X and Y position (Fig. 4). Additionally, the seam could be configured without internal travel moves, minimizing the visibility of transitions and improving the aesthetic quality of the printed part.

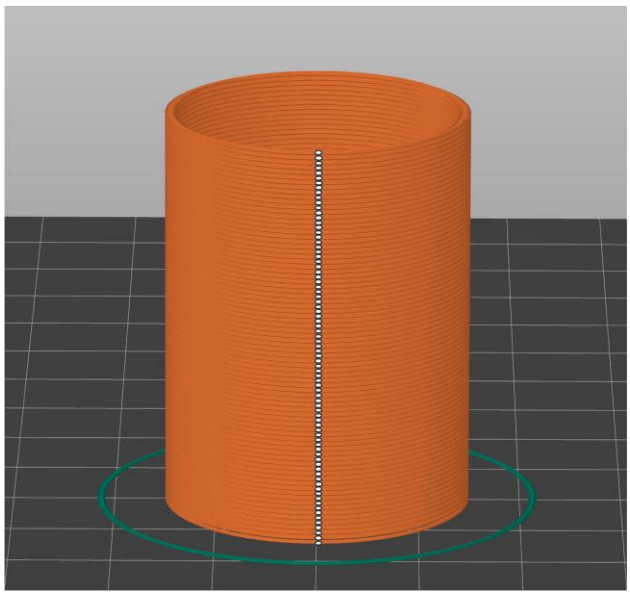

Fig. 4: Seam settings in Prusa Slicer

The cylinders printed using robotic additive manufacturing with G-code generated in the UltiMaker CURA slicer are shown in Figure 5 a) and b). The cylinders printed using G-code generated in Prusa Slicer are presented in Figure 5 c) and d). A solid 3D-CAD model was used for path planning in the printed sample shown in Fig. 5 a), while a hollow 3D-CAD model was used for the printed sample in Fig. 5 b)

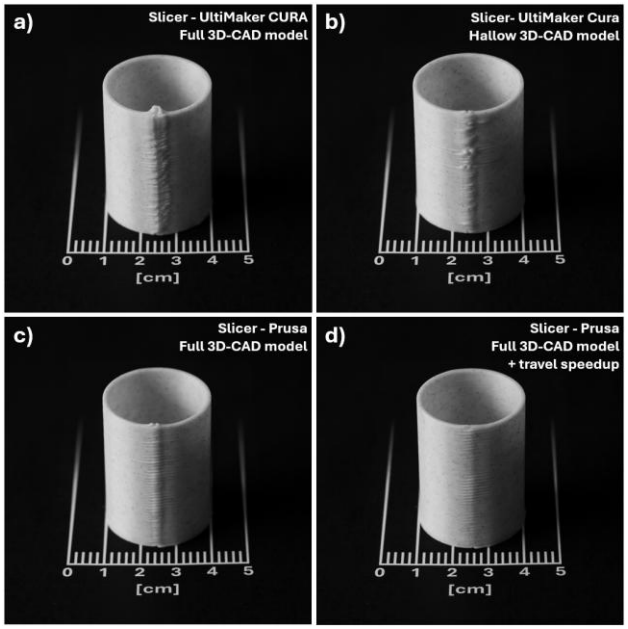

Fig. 5: Experiment 2 – Seam results
a) Slicer - UltiMaker CURA Full 3D-CAD model,
b) Slicer- UltiMaker Cura Hallow 3D-CAD model,
c) Slicer – Prusa Full 3D-CAD model,
d) Slicer – Prusa Full 3D-CAD model + travel speedup

For all experiments focused on seam optimization, the nozzle cooling was consistently set to 50%. All printed samples shown in Figure 5 were produced with a constant robot motion speed of 30 mm/s. In the case of the last print,

shown in Figure 5 (d), the travel movement speed was increased to 60 mm/s. This adjustment significantly contributed to achieving the highest observed seam quality, effectively minimizing unwanted defects.

3.3 Experiment 3 – Speed

In this experiment, the motion speed of the industrial robot was modified. The tested motion speeds were V10, V20, V30, and V40. The "V" (number) notation is used in ABB robots within the RAPID programming language and corresponds to speed in mm/s. It was essential to adjust the material feeding speed accordingly to avoid undesired effects such as overextrusion (excessive material deposition) at high feed rates or underextrusion (insufficient material deposition) at low feed rates. These deficiencies are visually demonstrated in Figure 6, where the differences in print quality at various speed settings are clearly observable.

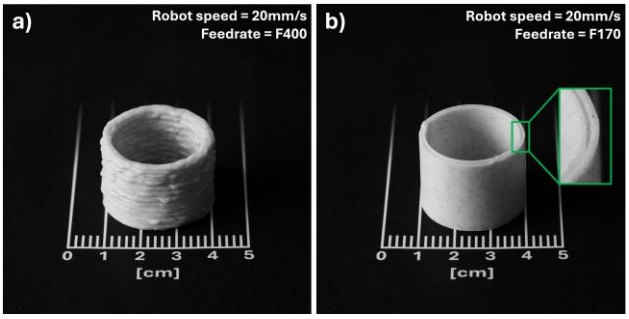

Fig. 6: Overextrusion and underextrusion
a) example of overextrusion, b) example of underextrusion

In the case of overextrusion, excessive material deposition caused material overflow along the edges of the printed part (Fig. 6 a)). Conversely, underextrusion resulted in an insufficient amount of extruded material, which could either lead to a complete print failure or, in a better scenario, gaps between the perimeter walls, as shown in Figure 6 b).

The material feeding speed was controlled through the print head settings using the F(number) command, where the numerical value F represents the material feed rate in mm/min. For instance, an F400 setting corresponds to a feed rate of 400 mm/min, which, when converted to seconds, equals approximately 6.666 mm/s (400/60).

Cooling was maintained at a constant 50% throughout this experiment. The resulting printed samples, produced at different robot motion speeds, are presented in Fig. 7. The robot's printing speeds for each experimental sample are indicated in the corresponding images. For travel movements between samples, the robot's speed was increased by approximately +200% compared to the printing speed. For example, when the robot's printing speed was set to V20, the travel speed was increased to V60.

Interesting results were also observed in terms of dimensions of the wall width of the printed part and the overall diameter of the printed cylinder. These dimensions were significantly influenced by the material feeding speed, which was adjusted according to the motion speed of the industrial robot. A secondary influencing factors could be the centripetal and centrifugal forces acting during the deposition of individual layers of the rotational part, particularly at higher robot speeds. However, these forces would likely not play a significant role in printing non-circular linear parts, where the rotational characteristics of layering would not be present during robot motion.

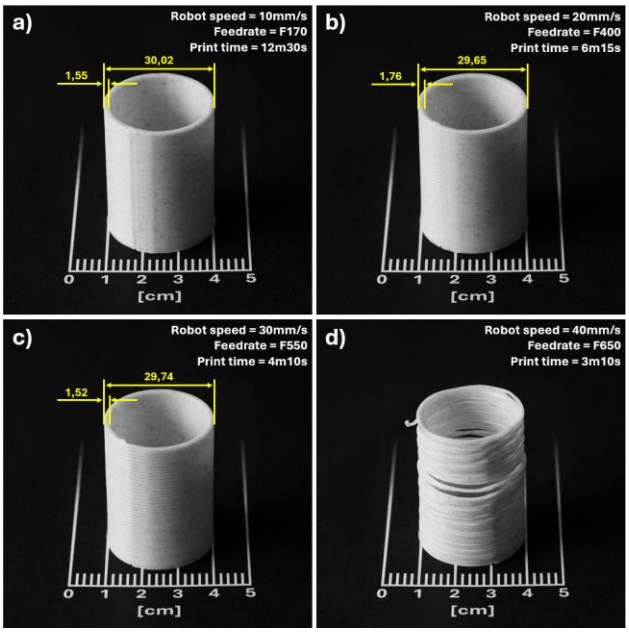

Fig. 7: Experiment 3 – Speed results
a) robot speed V10, b) robot speed V20,
c) robot speed V30, d) robot speed V40

The maximum robot motion speed at which an acceptable print quality was maintained was V30. At V40, successful print completion was no longer possible. At this speed, with cooling set to 50%, delamination occurred, similar to sample shown in Fig. 2 d), but in this case, it was due to insufficient material melting at a high feed rate. When the fan power was reduced to 20%, delamination persisted and was further accompanied by irregular waviness in the deposited layers, as illustrated in Fig. 7 d).

Printing tasks were successfully completed at robot speeds of V10, V20, and V30. The most significant difference between them was the total print time. However, at V30, a notable issue was observed in the quality of layer transitions, as discussed in the previous seam experiment (Fig. 7 c)). The best visual print quality was achieved at V20, as seen in Fig. 7 b).

3.4 Experiment 4 – perimeters

In conventional printing with infill, it is possible to adjust the infill pattern, density, and the number of perimeter layers. In the case of thin-walled tubes printed in this experiment, the structures were printed without infill, with their geometry consisting of one or multiple perimeter layers. The wall thickness of the printed parts directly depends on the number of perimeters, the nozzle diameter, the overlap of individual layers, and the material feed rate, which is adjusted to match the robot's movement speed.

For this experiment, a 1 mm nozzle was used. In future research, larger nozzle diameters are planned for large-format robotic additive manufacturing. The resulting printed samples, produced with one, two, and four perimeters, are shown in Fig. 7. All samples were printed at a robot movement speed of V20 with cooling set to 50%.

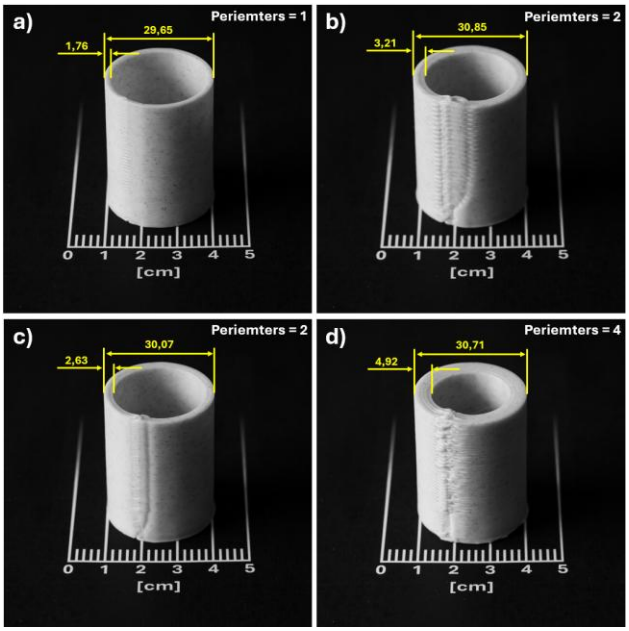

Fig. 8: Experiment 4 – Perimeters results
a) 1 perimeter, b) 2 perimeters,
c) 2 perimeters + higher feedrate, d) 4 perimeters

In the previous experiment, the most suitable speed was identified as V20 with a material feed rate of F400. However, using the same settings for printing two perimeters (Fig. 8 b)) resulted in a significantly poor-quality seam and an excessively thick wall. A better result was achieved by reducing the material feed rate to F300 (Fig. 8 c)). With this adjustment, the wall thickness was measured at 2.63 mm, the overall dimensions were 30.07 mm and a significantly improved seam quality was visually observed.

However, printing a cylinder with four perimeters presented challenges. Due to the continuous, uninterrupted material feed and the frequent transitions between perimeters and layers occurring at the same location, excessive material deposition occurred. This led to defects visible in Fig. 8 d).

3.5 Further Experiments

In the future, we plan to expand our experiments beyond planar thin-walled tube printing to include the additive manufacturing of curved tubes using a non-planar printing. The realization of such printing task requires specialized path planning for the industrial robot, with a focus on dynamical adaptation of the print head orientation. This approach will enable a more effective utilization of robotic additive manufacturing for producing complex geometries.

In the current research, the Siemens NX software environment was used for path planning in the initial experiments. The practical execution of the printing task with the generated paths is shown in Figure 9. The printing parameters used were consistent with those presented in this article: cooling was set to 50%, the robot motion speed was V10, the material feed rate was F170, and the printed geometry consisted of a single perimeter. Regarding hardware, software, and constant parameters, they remained identical to those specified in this article and shown in Tables 1 and 2.

The printing process and the initial experimental samples are illustrated in Figure 8. During this printing process, it was necessary to dynamically adjust the orientation of the print head.

4 CONCLUSION

This study focused on path planning and the optimization of key parameters for robotic additive manufacturing (RAM) of thin-walled tubes using an ABB IRB 120 industrial robot and an FDM print head. The experiments analyzed and optimized critical parameters influencing print quality, including cooling, robot motion speed, material feed rate, and the number of perimeters.

The key findings and recommendations based on the experimental results are as follows:

- Optimal Print Quality: The best print quality was achieved at a robot motion speed of V20 and a material feed rate of F300–F400, depending on the number of perimeters.
- Cooling Significance: Proper cooling of the print head was identified as a crucial factor, especially at higher motion speeds. Improper cooling settings at V30 and above led to reduced print quality and layer delamination.
- Printing with Multiple Perimeters: When printing tubes with multiple perimeters, precise adjustment of the material feed rate and careful optimization of the transition trajectory between layers were necessary to avoid defects in the seam location.
- Future Work – Non-planar Printing: Future research will focus on the printing of non-planar curved tubes, requiring advanced path planning and synchronization of the print head orientation with the geometry of the printed structure.

The findings of this study represent a significant step toward more efficient and precise robotic additive manufacturing with optimized printing parameters for thin-walled parts.

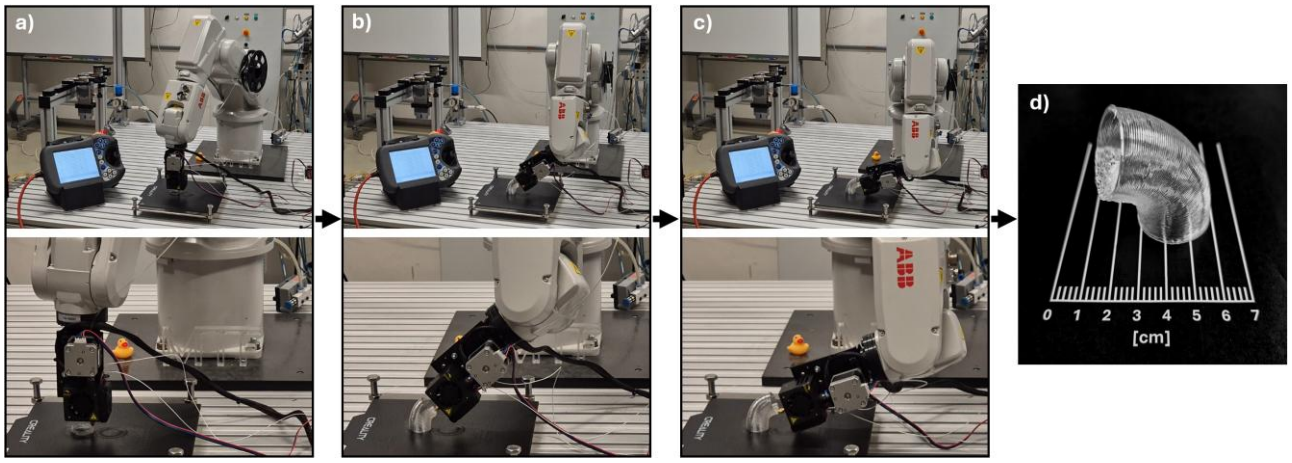

Fig. 9: Process of robotic additive manufacturing of thin-walled curved tubes
a), b), c) Steps of process, b) Initial experimental print

ACKNOWLEDGEMENT

This work was funded by the Grant Scheme for Supporting Excellent Teams of Young Researchers under internal project number 1353, titled "Research on path generation and motion planning of industrial robot and its use in hybrid manufacturing with MEX technology and subtractive processes."

Additionally, this research was supported by the project APVV-23-0084 "Robotic-Based Hybrid Manufacturing of Workpieces for the Concept of Smart Production" funded by the Slovak Research and Development Agency.

5 REFERENCES

[Abdulhameed 2019] Abdulhameed, O., Al-Ahmari, A., Ameen, W., and Mian, S. H. Additive manufacturing: Challenges, trends, and applications. Advances in Mechanical Engineering, 2019, vol. 11(2), pp. 1–27. doi: 10.1177/1687814018822880

[Bhatt 2020] Bhatt, P. M., Malhan, R. K., Rajendran, P., and Gupta, S. K. Building free-form thin shell parts using supportless extrusion-based additive manufacturing. Additive Manufacturing, 2020, vol. 32. doi: 10.1016/j.addma.2019.101003

[Bryła 2021] Bryła, J., and Martowicz, A. Study on the importance of a slicer selection for the 3d printing process parameters via the investigation of g-code readings. Machines, 2021, vol. 9(8), pp. 18. doi: 10.3390/machines9080163

[Fry 2020] Fry, N. R., Richardson, R. C., and Boyle, J. H. Robotic additive manufacturing system for dynamic build orientations. Rapid Prototyping Journal, 2020, vol. 26(4), pp. 659–667. doi: 10.1108/RPJ-09-2019-0243

[Geuy 2023] Geuy, M., Martin, J., Simpson, T., and Meisel, N. Path Planning for Non-Planar Robotic Additive Manufacturing. Solid Freeform Fabrication 2023: Proceedings of the 34th Annual International Solid Freeform Fabrication Symposium – An Additive Manufacturing Conference, 2023, pp. 865–880.

[Hajare 2022] Hajare, D. M., and Gajbhiye, T. S. Additive manufacturing (3D printing): Recent progress on advancement of materials and challenges. Materials Today: Proceedings, 2022, vol. 58(2022), pp. 736–743. doi: 10.1016/j.matpr.2022.02.391

[Huang 2019] Huang, Y., Carstensen, J., Tessmer, L., and Mueller, C. Robotic Fabrication in Architecture with Nonstandard Topology Robotic Fabrication in Architecture, Art and Design 2018 2019,. Springer International Publishing. doi: 10.1007/978-3-319-92294-2

[Kubalak 2016] Kubalak, J. R., Mansfield, C. D., Pesek, T. H., Snow, Z. K., Cottiss, E. B., Ebeling-Koning, O. D., Price, M. G., Traverso, M. H., Tichnell, L. D., Williams, C. B., Wicks, A. L. Design and realization of a 6 degree of freedom robotic extrusion platform. Solid Freeform Fabrication 2016: Proceedings of the 27th Annual International Solid Freeform Fabrication Symposium - An Additive Manufacturing Conference, SFF 2016, 2016, pp. 1314–1332.

[Li 2024] Li, X., Liu, W., Hu, Z., He, C., Ding, J., Chen, W., Wang, S., Dong, W. Supportless 3D-printing of non-planar thin-walled structures with the multi-axis screw-extrusion additive manufacturing system. Materials & Design, 2024, vol. 240. doi: 10.1016/j.matdes.2024.112860

[Miri 2022] Miri, S., Kalman, J., Canart, J. P., Spangler, J., and Fayazbakhsh, K. Tensile and thermal properties of low-melt poly aryl ether ketone reinforced with continuous carbon fiber manufactured by robotic 3D printing. International Journal of Advanced Manufacturing Technology, 2022, vol. 122(2), pp. 1041–1053. doi: 10.1007/s00170-022-09983-7

[Rasiya 2020] Rasiya, G., Shukla, A., and Saran, K. Additive Manufacturing - A Review. Materials Today: Proceedings, 2020, vol. 47, pp. 6896–6901. doi: 10.1016/j.matpr.2021.05.181

[Safeea 2022] Safeea, M., Bearee, R., and Neto, P. An integrated framework for collaborative robot assisted additive manufacturing. Journal of Manufacturing Processes, 2022, vol. 81, pp. 406–413.

[Shah 2022] Shah, A. Emerging trends in robotic aided additive manufacturing. Materials Today: Proceedings, 2022, vol. 62(P13), pp. 7231–7237. doi: 10.1016/j.matpr.2022.03.680

[Singh 2022] Singh, G., and Banga, V. K. Robots and its types for industrial applications. Materials Today: Proceedings, 2022, vol. 60, pp. 1779–1786. doi: 10.1016/j.matpr.2021.12.426

[Sljivic 2019] Sljivic, M., Pavlovic, A., Kraisnik, M., and Ilic, J. Comparing the accuracy of 3D slicer software in printed enduse parts. IOP Conference Series: Materials Science and Engineering, 2019, vol. 659 (1). doi: 10.1088/1757-899X/659/1/012082